

Configuration weight function method to solve the many-body Schrödinger equation.

V.M.Tapilin^{1, a)}

Boreskov Institute of Catalysis, Novosibirsk 630090, Russia

(Dated: 31 March 2022)

A method to solve the Schrödinger equation based on the use of constant particle-particle interaction potential surfaces is proposed. The many-body wave function is presented in configuration interaction form with coefficients - configuration weight functions - dependent on the total interaction potential. A set of linear ordinary differential equations for the configuration weight functions was developed and solved for particles in a infinite well and He-like ions. The results demonstrate that the method is variational and provides upper bound for energy of the ground state; even in its lowest two-body interaction potential surfaces approximation, it is more accurate than the conventional configuration interaction method and demonstrates a better convergence with a basis set increase. For He-like ions one configuration approximation with non-interaction electrons functions are used as basis set the calculated energies are below the Hartree-Fock limit. In three configuration approximations the accuracy of energy calculation is close to CI accuracy with 35 configuration taking into account. Four configurations give the energies below CI method and slightly below precise calculation with Hylleraas type wave functions.

I. INTRODUCTION

Møller-Plesset perturbation theory and configuration interactions are the conventional methods of treating electron-electron correlation in the theory of atoms and molecules¹. Unfortunately, both of them due to the presence of the correlation cusp^{2,3} in the wave function reveal slow convergence of electron energy with basis set increasing. At the same time, the fast growth of computational work which is mainly related to the need for calculation of four-index two-electron integrals, places a hard limit the basis set size.

Density functional theory (DFT)⁴⁻⁷ is another approach to solve quantum many-body problem. Based on the solution of Kohn-Sham equations⁵, it has been successfully applied to many problems⁷. Unfortunately, the exact form of this functional is unknown, and its approximated forms do not always provide the required accuracy, for example, in treating systems with strong electron-electron correlations⁸⁻¹⁰.

All of these give reasons for a search other ways of treating the correlation problem. To speed up the convergence, explicitly correlated R12 and F12 methods have been developed over the last two decades¹¹⁻²⁸. Following to Hylleraas^{29,30} and Boys and Handy,^{31,32} these methods are based on representation of the wave function as a production of one-particle wave functions and a correction function explicitly depending on electron-electron spacing. In R12 the correction function linearly depends on electron-electron spacing^{11,12}, in F12 this dependence is exponential²¹. Iterative complement interaction method has been formulated in^{33,34}. This paper is aimed at de-

veloping another way of treating the correlation problem presented in.³⁵ The theory is based on the introduction of constant particle-particle interaction potential surfaces. It follows directly from the definition of such surfaces that particle-particle interaction acts along the normal to the surface and, therefore, does not influence particle motion on the surface. Thus this motion can be described by a wave function of independent particles, which results in a new exact representation for many-body wave function and a set of equation to determining it. Further a new form of many-body wave function and equations to find it will be proposed and applied to particles in a infinite square well and He-like ions.

II. CONFIGURATION WEIGHT FUNCTIONS AND EQUATIONS DETERMINING THEM

Consider the Schrödinger equation of n interacting particles

$$H\Psi = (H_0 + V_{int})\Psi = E\Psi, \quad (1)$$

where H_0 is the kinetic energy and external field operator, and V_{int} particle-particle interaction operator

$$H_0(\mathbf{R}) = \sum_{i=1}^n \left[-\frac{1}{2}\nabla_i^2 + V(\mathbf{r}_i) \right] = -\frac{1}{2}\nabla_{\mathbf{R}}^2 + V(\mathbf{R}), \quad (2)$$

$$V_{int}(\mathbf{R}) = \frac{1}{p(\mathbf{R})} = \sum_{i=1}^{n-1} \sum_{j>i}^n \frac{1}{r_{ij}} = \sum_{i=1}^{n-1} \sum_{j>i}^n v_{ij}. \quad (3)$$

Here \mathbf{R} stands for a set of particle coordinates $\mathbf{r}_1, \dots, \mathbf{r}_n$, $r_{ij} = |\mathbf{r}_i - \mathbf{r}_j|$.

A constant interaction potential surface $V_{int}(\mathbf{R}) = 1/p$ selects a subspace of particle coordinates in which particles motion is correlated *ab origin* due to the demand

^{a)}Electronic mail: tapilin@catalysis.ru

remaining at the surface rather than particle interaction. The resulting interaction force, acting at the interacting particles on the surface, directs along the normal to the surface and does not act on particle movement along the surface, giving rise to redistribution of the particles between surfaces only. Thus, the eigenfunctions of (2)

$$\Phi_{\mathbf{i}}(\mathbf{R}) = \widehat{P}\phi_{i_1}(\mathbf{r}_1) \dots \phi_{i_n}(\mathbf{r}_n) \quad (4)$$

where \widehat{P} is an operator symmetrizing wave function according to the system spin, satisfies of (1) on the constant interaction potential surface with eigenvalues

$$\epsilon_{\mathbf{i}} = \epsilon_{i_1} + \dots + \epsilon_{i_n} + 1/p. \quad (5)$$

Here we introduced vectors \mathbf{i} with components i_1, \dots, i_n . Function (4) does not satisfy to (1) in the whole space due to a particle redistribution from surface to surface owing to changing p . We represented the function satisfying (1) in the form

$$\Psi(\mathbf{R}) = \sum_{\mathbf{i}} \chi_{\mathbf{i}}(p(\mathbf{R})) \Phi_{\mathbf{i}}(\mathbf{R}). \quad (6)$$

Function (6) has the form of configuration interaction function in which coefficients are replaced by functions $\chi_{\mathbf{i}}(p(\mathbf{R}))$ depending on interaction potential at points \mathbf{R} . This function determines the contributions of different configurations for each constant interaction potential surface p and hereinafter referred to as *configuration weight function*. Here and below functions χ and Φ without subscripts mean vector functions with the components $\chi_{\mathbf{i}}$ and $\Phi_{\mathbf{i}}$ respectively.

The result of action of Laplace operator at function (6) can be written as

$$\begin{aligned} \nabla_i^2 \Psi(\mathbf{R}) &= \Phi(\mathbf{R}) \nabla_i^2 \chi(p(\mathbf{R})) + \\ &2 \nabla_i \chi(p(\mathbf{R})) \nabla_i \Phi(\mathbf{R}) + \chi(p(\mathbf{R})) \nabla_i^2 \Phi(\mathbf{R}) = \\ &\Phi(\mathbf{R}) (\nabla_i p)^2 \frac{d^2 \chi(p)}{dp^2} + [\Phi(\mathbf{R}) \nabla_i^2 p \\ &+ 2 \nabla_i p \nabla_i \Phi(\mathbf{R})] \frac{d\chi(p)}{dp} + \chi(p) \nabla_i^2 \Phi(\mathbf{R}), \end{aligned} \quad (7)$$

where results of ∇ operator action on collective variable p are

$$\nabla_i p = -\frac{1}{V_{int}^2} \nabla_i V_{int} = p^2 \sum_{j>i} \frac{\mathbf{r}_{ij}}{r_{ij}^3}, \quad (8)$$

$$\begin{aligned} (\nabla_i p)^2 &= p^4 \sum_{j>i, k>i} \frac{\cos \langle \mathbf{r}_{ij}, \mathbf{r}_{ik} \rangle}{r_{ij}^2 r_{ik}^2} \\ &= p^4 \sum_{j>i, k>i} \frac{r_{ij}^2 + r_{ik}^2 - r_{jk}^2}{r_{ij}^3 r_{ik}^3}, \end{aligned} \quad (9)$$

$$\nabla_i^2 p = \frac{2}{V_{int}^3} (\nabla_i V_{int})^2 - \frac{1}{V_{int}^2} \nabla_i^2 V_{int} = \frac{2}{p} (\nabla_i p)^2. \quad (10)$$

In (10) it was taken into account that the Coulomb potential is satisfied to the Laplace equation.

Determining matrix \mathbf{F} of any operator \widehat{F} on a surface p by matrix elements

$$F_{\mathbf{ij}}(p) = \langle \Phi_{\mathbf{i}} | \widehat{F} | \Phi_{\mathbf{j}} \rangle_p = \int_{\mathbf{S}(p)} d\mathbf{R} \Phi_{\mathbf{i}} \widehat{F} \Phi_{\mathbf{j}} \quad (11)$$

The expression for energy in this notation can be written in the form

$$E = \frac{\int dp \chi^{tr}(p) \mathbf{H}(p) \chi(p)}{\int dp \chi^{tr}(p) \mathbf{S}(p) \chi(p)}. \quad (12)$$

where \mathbf{H} and \mathbf{S} are the Hamiltonian and overlap matrices, χ^{tr} means the transpose of column vector function χ . It should be noted that functions $\Phi_{\mathbf{i}}$, orthogonal in the whole space, can be unorthogonal on a surface. Moreover, the set of functions which are linear independent in the whole space can become linear dependent on the surface.

Energy minimization in respect to $\chi_{\mathbf{i}}$ leads to equations

$$\begin{aligned} -\frac{\mathbf{T}(p)}{2} \frac{d^2 \chi(p)}{dp^2} - \left(\frac{\mathbf{T}(p)}{p} + \frac{\mathbf{U}(p)}{2} \right) \frac{d\chi(p)}{dp} \\ + \left(\mathbf{H}_0(p) + \frac{\mathbf{S}(p)}{p} \right) \chi(p) = E \mathbf{S}(p) \chi(p), \end{aligned} \quad (13)$$

where

$$T_{\mathbf{ij}}(p) = \langle \Phi_{\mathbf{i}}(\mathbf{R}) | (\nabla_i p)^2 | \Phi_{\mathbf{j}}(\mathbf{R}) \rangle_p, \quad (14)$$

$$U_{\mathbf{ij}}(p) = \langle \Phi_{\mathbf{i}}(\mathbf{R}) | \nabla_i p \nabla_i | \Phi_{\mathbf{j}}(\mathbf{R}) \rangle_p, \quad (15)$$

$$H_{0, \mathbf{ij}}(p) = \langle \Phi_{\mathbf{i}}(\mathbf{R}) | H_0(\mathbf{R}) | \Phi_{\mathbf{j}}(\mathbf{R}) \rangle_p \quad (16)$$

$$S_{\mathbf{ij}}(p) = \langle \Phi_{\mathbf{i}}(\mathbf{R}) | \Phi_{\mathbf{j}}(\mathbf{R}) \rangle_p. \quad (17)$$

Matrices $\mathbf{U}(p)$ and $\mathbf{H}_0(p)$ containing Φ derivatives are nonsymmetric. It is easy to obtain

$$\mathbf{H}_0(p) = \begin{pmatrix} \epsilon_1 S_{11}(p) & \epsilon_2 S_{12}(p) & \dots & \epsilon_{n_f} S_{1n_f}(p) \\ \epsilon_1 S_{21}(p) & \epsilon_2 S_{22}(p) & \dots & \epsilon_{n_f} S_{2n_f}(p) \\ \dots & \dots & \dots & \dots \\ \epsilon_1 S_{n_f 1}(p) & \epsilon_2 S_{n_f 2}(p) & \dots & \epsilon_{n_f} S_{n_f n_f}(p) \end{pmatrix} \quad (18)$$

Obviously after integration over p matrices \mathbf{S} and \mathbf{H}_0 become diagonal with matrix elements $S_{ij} = \delta_{ij}$ and $H_{0, ij} = \epsilon_i \delta_{ij}$, \mathbf{U} becomes symmetric. Matrices $\mathbf{H}_0(p)$ and $\mathbf{H}_0^{tr}(p)$ have the same eigenvalues ϵ_i . It should be noted that artificial symmetrization of $\mathbf{H}_0(p)$ by sum of $\mathbf{H}_0(p)$ and $\mathbf{H}_0^{tr}(p)$ leads to incorrect results even for non-interaction particles.

Eq. (13) is a set of linear ordinary differential equation with eigenvalues equal to the system energy. The terms containing derivatives of χ describe additional contributions to kinetic energy, arising when redistribution of electrons between different interaction potential surfaces occurs. There is no such redistribution for non-interacting particles. For this case functions (4) are eigenfunctions of \mathbf{H} , functions $\chi(p)$ do not depend on p and differential equations (13) reduce to the Schrödinger equations of non-interacting particles. Due to asymmetry of matrices in (13) besides configuration weight function

$\chi(p)$ there is another set of configuration function χ^l (superscript l means 'left'), which is a solution of Eq. (13) with transposed matrices.

The boundary conditions for χ follow from the demand for Ψ to be finite in the whole space. At $p = 0$ at least two particles are at the same space point. In the neighborhood of such points, as it was shown in², the wave function behaves as $e^{r_{12}/2}$, which means that the 1st derivative of the wave function is discontinuous at such points, giving rise to the cusp problem - slow convergence of the wave function to the exact one with increasing the basis set. Consistent with our theory there is no cusp problem at all because points of the wave function discontinuity are lying at the boundary point. To find the boundary conditions at $p = 0$ rewrite (9) in the form

$$(\nabla_i p)^2 = p^4 \left(\sum_{j>i} \frac{1}{r_{ij}^4} + \sum_{k>i} \frac{\cos \langle \mathbf{r}_{ij}, \mathbf{r}_{ik} \rangle}{r_{ij}^2 r_{ik}^2} \right) \quad (19)$$

and expand (19) into the Taylor series. The expansion can be performed for two, three etc. particles at the same point, however, in all cases the results will be the same

$$(\nabla_i p)^2 = 1 + O(r_{12}) \quad (20)$$

so when $p \rightarrow 0$ (13) reduced to 1st order differential equations

$$-\frac{\mathbf{S}(p)}{p} \frac{d\chi(p)}{dp} + \frac{q\mathbf{S}(p)}{p} \chi(p) = 0, \quad (21)$$

with a restricted at $p = 0$ solutions

$$\chi_i(p) = \chi_i(0) e^{qp/2} \quad (22)$$

The wave function behavior (22) coincide with $e^{r_{12}/2}$ presented in paper². Eqs. (22) provide us with the bounder conditions at $p = 0$.

For $p \rightarrow \infty$ the interaction vanish and according to (8)-(10) matrices $\mathbf{S}^{-1}\mathbf{T}$, $\mathbf{S}^{-1}\mathbf{U}$, and $\mathbf{S}^{-1}\mathbf{H}_0$ tends to constant, so a solution of (13) can be approximated at a point p as $e^{\lambda p}$. Substitution of this representation in (13) leads to

$$\sum_{j=1}^{n_f} [-\lambda^2 T_{ij}(p)/2 - \lambda((T_{ij}(p)/p + U_{ij}(p)) + H_{0;ij}(p) + S_{ij}(p)/Zp - ES_{ij}(p))] \chi_j(p) = 0, \quad i = 1, \dots, n_f, \quad (23)$$

n_f is the number of configurations taken into account. Set (23) has non-zero solution if

$$\det(\Lambda) = 0 \quad (24)$$

where matrix Λ is determined by the expressions in the square brackets of (23). Obviously, $\det(\Lambda)$ is a $2n_f$ order polynomial of λ . The $2n_f$ roots of the polynomial, possibly complex, will be denoted λ_i . Not all of the roots

have physical meaning. The demand that wave function must be finite in the whole space leads to

$$\chi_i(p) S_{ij} \chi_j(p) \approx e^{\lambda_i(p) + \lambda_j(p)} S_{ij} < \infty \quad (25)$$

Another restriction on the choice of physical meaning $\chi_i(p)$ results from demand that with the switch off the particle-particle interaction $\chi_i(p)$ becomes constant, so $\lambda_i(p) \rightarrow 0$ when $q \rightarrow 0$. As a result, the number of physical meaning $\lambda_i(p)$ does not exceed n_f . The demand (25) provide us the with bounder condition for (13) for a big p .

III. CONSTANT INTERACTION POTENTIAL SURFACES AND THEIR APPROXIMATIONS

In case of two particles the constant interaction potential surface is a sphere of radius r_{12} with the center at the position of the selected particle. In case of n -particles the values r_{1i} , $i = 2, \dots, n$, determine $n - 1$ spheres remaining on which particles do not change the interaction potential with the first one; even the total potential will change. Setting r_{2i} , $i = 3, \dots, n$, to save interaction potential with the first two particles the rest of the particles must move along the circles of radius $\rho_i = r_{1i} \sin v_{1i}$ obtained by the crossing lines of the spheres and planes $z_i = r_{1i} \cos v_{1i}$, $\cos v_{1i} = (r_{1i}^2 + r_{12}^2 - r_{2i}^2)/2r_{12}r_{1i}$, in a coordinate system with z -axes directed along \mathbf{r}_{12} . The values r_{2i} are not arbitrary but must satisfy the conditions

$$|r_{1i} - r_{12}| \leq r_{2i} \leq r_{1i} + r_{12}. \quad (26)$$

Setting r_{3i} , $i = 4, \dots, n$ determines two points at the circles with coordinates

$$z_i = r_{1i} \cos v_{1i}, \quad y_i = \rho_i \cos \varphi_i, \quad x_i = \pm \rho_i |\sin \varphi_i|. \quad (27)$$

where $\cos \varphi_i = (\rho_i^2 + \rho_3^2 + (z_i - z_3)^2)/2\rho_i\rho_3$. The values of r_{3i} must satisfy to inequalities

$$(\rho_i - \rho_2)^2 + (z_i - z_2)^2 \leq r_{3i}^2 \leq (\rho_i + \rho_2)^2 + (z_i - z_2)^2. \quad (28)$$

The set of r_{ij} with $i \leq 3$ and $j > i$ values determines a solid polyhedron with the particles at its vertexes, which is a point at a constant interaction potential surface, shown for four particles in Fig.1. Rotation of the polyhedron around of \mathbf{r}_{12} axes, rotation of the axes around \mathbf{r}_1 point and the move of the point in the space determine a constant interaction potential surface. The averaging of any one-body operator \hat{F} along the surface can be expressed as

$$F(p) = \int d\mathbf{r}_1 \int r_{12}^2 \sin v_{12} d\varphi_2 dv_{12} \int r_{13} \sin v_{13} d\varphi_3 \Phi(\mathbf{r}_1, \dots, \mathbf{r}_n) \hat{F} \Phi(\mathbf{r}_1, \dots, \mathbf{r}_n) \quad (29)$$

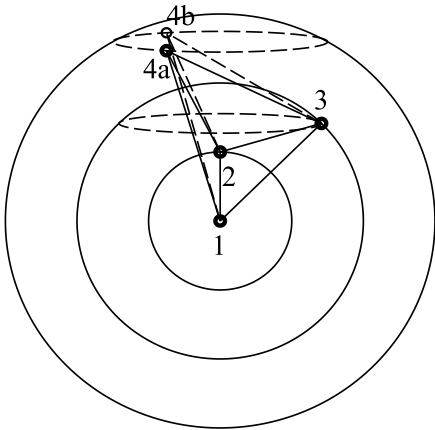


FIG. 1. A four particle tetrahedron. Particles (small numerated circles) are placed at the framework vertexes, the length of the framework edges equals to r_{ij} . Solid circles are sphere cross-section by $x = 0$ plane, dash curves are circles obtained by crossing spheres by $z_i = r_{1i} \cos \nu_{1i}$ planes, 4a and 4b points correspond to two points in (27)

where \mathbf{r}_i is determined by (26)-(28). So, $3(n-1)$ values r_{ij} with $i \leq 3$ and $j > i$, definitely determine the value of particle-particle interaction potential.

There are different combinations of r_{ij} with $i \leq 3$ and $j > i$ giving the same value of the interaction potential. As one can see from (3), the constant electron-electron interaction potential surface is a plane in the space of the pair potentials $\{v_{ij}\}$, which will be referred to as *v-space*. The usual space in which particles move will be referred to as *r-space*. The dimensionality of v-space is $n(n-1)/2$, however the restrictions introduced in the above paragraph reduced it to $3(n-1)$. Any point on a constant interaction potential surface v can be moved to surface v' by coordinate scaling

$$r_{ij}(v') = r_{ij}(v)v/v' \quad (30)$$

It means that it is enough to construct only one surface, for example,

$$v(v_{12}, \dots, v_{N-1, N}) = 1 \quad (31)$$

and obtain the other ones by scaling transformation (30).

Each point of v-space determines the relative particle positions r_{ij} in the r-space, so the set of \mathbf{R} belonging to the same surface can be easily determined. However, due to the multidimensionality of the plane and disability to integrate over the variables on the plane independently a numerical integration over the surface can be performed only for several particle systems. It means that in practice the developed theory can be applied only for such systems, and an extension of the theory to bigger systems needs to be simplified. Possible simplifications are proposed below.

At first, a constant potential surface for potential acting on a particle from the other ones can be introduced.

For one particle at \mathbf{r}_1 it consists of $n-1$ spheres of radius r_{1i} . Separate this potential from the total one

$$\frac{1}{p_1} = \sum_i \frac{1}{r_{1i}}, \quad (32)$$

and determining matrix elements of a operator \hat{F}

$$F(r_{12}, \dots, r_{1n}) = \int d\mathbf{r}_1 \int d\Omega_{12} \dots \int d\Omega_{1n}$$

$$\Psi^*(\mathbf{r}_1, \mathbf{r}_1 + \mathbf{r}_{12}, \dots, \mathbf{r}_1 + \mathbf{r}_{1n}) \hat{F} \Psi(\mathbf{r}_1, \mathbf{r}_1 + \mathbf{r}_{12}, \dots, \mathbf{r}_1 + \mathbf{r}_{1n}), \quad (33)$$

where $d\Omega_{1i} = r_{1i}^2 \sin(\theta_{1i}) d\theta_{1i} d\varphi_{1i}$, and integration over Ω_{1i} can be performed independently. As a result, the dimension of the constant potential surface becomes $n-1$.

Another possible way of such simplification is an introduction of a set of approximations to the theory based on the further lowering the dimension of interaction potential surface by averaging over the moving of a part of particles. Obviously, the averaging over all particles but one leads to Hartree-Fock approximation. The next approximation - averaging over all particles but two - describes the motion of exactly correlating particle pair in the middle field of other particles can be called *independent pair* approximation. The same way can be introduced *independent triplet*, *quadruple*, etc. approximations. As a result, one can obtain the set of equations (13) in which matrix elements are calculated as

$$F_{ij}(p_m) = \int_{S(p_m)} d\mathbf{R}_m \int d\mathbf{R}_{n-m} \Phi_i(\mathbf{R}) \hat{F} \Phi_j(\mathbf{R}), \quad (34)$$

where $1/p_m$ denotes potential and $S(p_m)$ is a constant interaction potential surface in the space of m particles. Integration over the rest $n-m$ particles can be performed independently for each particle coordinates. Operator \hat{F} can be represented as a sum of operators acting in space of m and $n-m$ particles, and interaction operator between these two spaces

$$\hat{F}(\mathbf{R}) = \hat{F}(\mathbf{R}_m) + \hat{F}(\mathbf{R}_{n-m}) + \hat{F}(\mathbf{R}_m, \mathbf{R}_{n-m}). \quad (35)$$

In accordance with this division, the total energy (12) can be represented as a sum of energies of m and $n-m$ particle systems and interaction energy between them. Obviously, energy of $n-m$ particle system does not take into account particle correlation. It gives the constant contribution in eigenvalues of (13). The interaction here plays the role of an external field acting on m -particle system. Thus (13) is reduced to a set of equations for m -particle in the external field and the middle field of other particles. The solutions of (13) gives an exactly correlated function for m particles in the environment described above.

IV. SIMPLE EXACTLY SOLVABLE EXAMPLES.

To test the theory we considered two simple models with directly solvable Schrödinger equation and solved the

equation directly, with configuration interaction method, and with different approximations of the developed theory. We considered two and three particles in a one dimensional infinite square potential well. To avoid errors in derivatives approximation by finite differences and to reduce the numerical calculations, we *ab origin* will use the discrete space. The model makes it possible to solve the Schrödinger equation directly. The comparison results obtained on the basis of the developed methods with the exact ones allows us to estimate the validity and efficiency of the theory.

The model Schrödinger equation

Represent the kinetic energy operator h acting at particle α as

$$h(x_\alpha) = -\frac{d^2\psi_i(x_\alpha)}{dx_\alpha^2} = \frac{2\psi_i(x_\alpha) - \psi_i(x_\alpha + \delta x_\alpha) - \psi_i(x_\alpha - \delta x_\alpha)}{\delta x_\alpha^2} \quad (36)$$

where x_α numerates the points in the well. Lets m is the number of such points. The eigen functions $\psi_i(x_\alpha)$ of operator (36) vanish at the boundary points of a infinite well are

$$\psi_i(x_\alpha) = \sqrt{\frac{2}{\pi}} \sin i x_\alpha, \quad x_\alpha = j \delta x_\alpha, \quad \delta x_\alpha = \pi/(m-1), \\ i = 1, \dots, m-2, \quad j = 0, \dots, m-1, \quad (37)$$

Functions (37) are a complete set of functions in the well. The Schrödinger equation for n particles in the well can be approximated as

$$H\Psi = \sum_{\alpha} [h(x_\alpha) + \sum_{\beta=\alpha+1}^n v(x_\alpha, x_\beta)]\Psi = E\Psi \quad (38)$$

where interaction potential between particles α and β was choose in the form

$$v(x_\alpha x_\beta) = \frac{q}{|x_\alpha - x_\beta| + \lambda} \quad (39)$$

where λ is added to interaction to avoid infinity when $x_\alpha = x_\beta$, q is particle's charge. The order of this set of equations is m^n , so for two and three particles in the well the orders are 64 and 512 correspondingly and solution of (38) can be obtained by direct diagonalization of matrix H . This solution will be a reference point in estimating the accuracy of approximated method to solve (38).

A solution of (38) Ψ can be represented by a linear combination of configuration functions $\Phi_{\mathbf{i}}$

$$\Psi(\mathbf{x}) = \sum_{\mathbf{i}} c_{\mathbf{i}} \Phi_{\mathbf{i}}(\mathbf{x}) \quad (40)$$

where \mathbf{i} and \mathbf{x} are n -dimensional vectors with components i_1, \dots, i_n and x_1, \dots, x_n , correspondingly, and Φ

is a production of one-body functions symmetrized with operator \hat{S}

$$\Phi_{\mathbf{i}}(\mathbf{x}) = \hat{S}\psi_{i_1}(x_1)\psi_{i_2}(x_2)\dots\psi_{i_n}(x_n) \quad (41)$$

where ψ_i is one particle functions. If ψ_i is a complete set of functions, (40) is an exact representation of the wave functions, in other cases (40) only approximates Ψ . Below we have compared the convergence of the approximated functions of configuration interaction (CI) and configuration weight function (CWF) methods.

In CI method (38) is transformed to

$$\sum_{\mathbf{i}_k} H_{\mathbf{i}_k \mathbf{j}_k} c_{\mathbf{j}_k} = E c_{\mathbf{i}_k} \quad (42)$$

where \mathbf{i}_k and \mathbf{j}_k are k -dimensioned vectors containing indexes only $k \leq m$ functions ψ_i , and

$$H_{\mathbf{i}\mathbf{j}} = \langle \Phi_{\mathbf{i}} | H | \Phi_{\mathbf{j}} \rangle \quad (43)$$

In CWF method the wave function has the form (40), but coefficients $c_{\mathbf{i}}$ are replaced by configuration weights functions $\chi_{\mathbf{i}}(p)$ which are dependent on the value of interaction potential

$$1/p = \sum_{\alpha, \beta > \alpha}^n v(x_\alpha, x_\beta) \quad (44)$$

and the weight functions satisfy to a set of equation

$$\sum_{\mathbf{i}_k} [H_{\mathbf{i}_k \mathbf{j}_k}(p) - E S_{\mathbf{i}_k \mathbf{j}_k}(p)] \chi_{\mathbf{j}_k}(p) = 0 \quad (45)$$

where

$$H_{\mathbf{i}_k \mathbf{j}_k}(p) = \langle \Phi_{\mathbf{i}_k} | H | \Phi_{\mathbf{j}_k} \rangle_p \quad (46)$$

$$S_{\mathbf{i}_k \mathbf{j}_k}(p) = \langle \Phi_{\mathbf{i}_k} | \Phi_{\mathbf{j}_k} \rangle_p \quad (47)$$

and summation is performed only over points x_α and x_β satisfying the condition (44) for a given p . Overlap matrix $S_{\mathbf{i}_k \mathbf{j}_k}(p)$ is appearing because functions $\Phi_{\mathbf{i}_k}$, orthogonal in the whole space, become non-orthogonal on subspaces determined by value p . As a results, the set of functions $\Phi_{\mathbf{i}_k}$ linear independent in the whole space may become linear dependent on a surface. In this case some of eigenvalues of matrix $S_{\mathbf{i}_k \mathbf{j}_k}(p)$ are equal to zero and we reduced the basis function set for these surfaces to exclude zero eigenvalues of the matrix.

Equations (45) are a representation in the discrete space of the equations (13) Indeed, kinetic energy operator acting in a discrete space at a product of the functions

$$\frac{\partial \chi(p(\mathbf{x})) \Phi(\mathbf{x})}{\partial x_\alpha} = [\chi(p(\mathbf{x}_\alpha, x_\alpha + \delta x_\alpha)) \Phi(\mathbf{x}_\alpha, x_\alpha + \delta x_\alpha) - \chi(p(\mathbf{x}_\alpha, x_\alpha - \delta x_\alpha)) \Phi(\mathbf{x}_\alpha, x_\alpha - \delta x_\alpha)] / (2\delta x_\alpha) \quad (48)$$

tends with $\delta x_\alpha \rightarrow 0$ to

$$\frac{\partial \chi(p(\mathbf{x}))}{\partial x_\alpha} \Phi(\mathbf{x}) + \chi(p(\mathbf{x})) \frac{\partial \Phi(\mathbf{x})}{\partial x_\alpha}$$

Table I. Energies of the ground and selected excited states of two particles in the infinite well for 1, 2, 3, and 8 ψ functions taking into account. SRF and CI columns contains the energies obtained with (45) and (42) equations, correspondingly. Relative errors are presented in the brackets.

state	2		3		4	8
	CWF	CI	CWF	CI	CI	CWF, CI, ext.
2	0.905666(4.10 ⁻⁴)	0.927756(2.10 ⁻²)	0.905284(2.10 ⁻⁶)	0.910008(5.10 ⁻³)	0.905968(8.10 ⁻⁴)	0.905282
3			1.511632(5.10 ⁻⁴)	1.536781(2.10 ⁻²)	1.519998(6.10 ⁻³)	1.510904
4	1.877636(3.10 ⁻²)		1.821044(6.10 ⁻⁵)	1.853396(2.10 ⁻²)	1.825807(3.10 ⁻³)	1.820939
5			2.217694(3.10 ⁻⁴)		2.248223(1.10 ⁻²)	2.216982
6			2.636500(4.10 ⁻²)		2.564415(2.10 ⁻²)	2.523710
8	3.065297(1.10 ⁻²)		3.033641(3.10 ⁻³)		3.060787(1.10 ⁻²)	3.023590
13	4.355834(2.10 ⁻³)		4.358194(1.10 ⁻³)			4.362801
21	5.644822(3.10 ⁻³)		5.696051(6.10 ⁻⁵)			5.664018
25	6.824136(8.10 ⁻³)		6.709824(7.10 ⁻⁵)			6.710304
28	7.779231(7.10 ⁻⁵)		7.779764(1.10 ⁻⁶)			7.779772

It should be note that kinetic energy operator is a hermitian operator for functions (41) in the whole space because the wave functions vanish at bounder points³⁶ and remains hermitian on the constant interaction potential surfaces for the same reason.

Equations (38), (42) and (45) have been solved for two and three particles in the well and the results are presented below.

Two particles in a infinite potential well

Energies of ground and some of excited antisymmetric stations for two particles in the wall are presented in Table I. States are numerated in compliance with the state numeration of H matrix. The results obtained with (42) and (45) for $k = 8$ coincide with the exact ones obtained by direct diagonalization of matrix H . The number of states obtained with CI method is equal to the antisymmetric functions $n_c = k(k - 1)$ which can be constructed with k one-body function. For CI states presented in Table I the corresponding states of CWF are also shown. However, the number of excited states calculated with CWF is grater than n_c because n_c states can be constructed for each constant interaction potential surface. Not all such constructed functions are linear independent which is revealed by appearing of zero eigenvalues of overlap matrix (47). In the calculations the number n_c has been reduced until all the eigenvalues become grater than zero. The growth of the number of linearly independent function with the increase the number of basis functions for CWF and CI are shown in Fig.2. The additional to CI excited states in Table I were chosen arbitrarily and show the accuracy of the calculated excited states energies.

Table I shows that the CWF relative energy error for $k = 2$ two order is less than the CI error. To reach comparable accuracy CI method needs $k = 4$ whereas

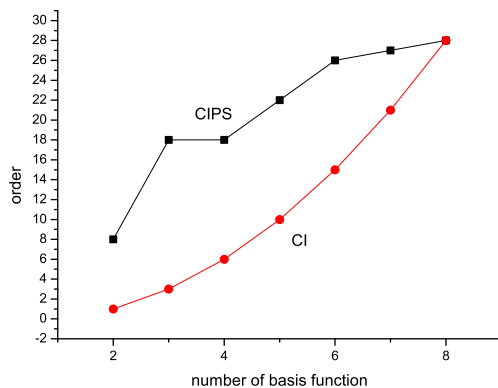


FIG. 2. Matrix order for CWF and CI

CWF gives practically exact energy for $k = 3$. Table I does not present the CWF results for $k = 4$ because they are coincide with those for $k = 3$ due to the equal number of independent configuration for these cases as it can be seen in Fig.2. The accuracy in energies of excited states at first drops with energy; than it starts to grow and at the end reaches the accuracy for the ground states.

Different convergence of CWF and CI methods reflects the different growth in the number of operated functions of these method. As one can see in Fig.2 for CWF the number of functions grows fast at the beginning and slows at the end whereas CI method shows a slow increase at the beginning and fast incise at the end.

Three particles in a infinite potential well

The main aim of solving a three particle model problem is to check the efficiency of different approximation to

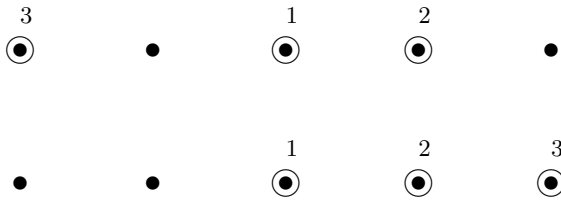


FIG. 3. Distinguish between surfaces. Numerated circles represent particles

exact interaction potential surfaces proposed in Part I. Just as in the previous section we solved the problem directly, by CI and CWF methods.

According to the value of the total interaction potential (39), all particle coordinate combinations for three particles in the well can be divided into twenty groups which we called constant interaction potential surfaces and designated below as p_t . Besides, we determined two other interaction potential surfaces, p_1 containing 36 surfaces and p_2 containing 8 surfaces. These surfaces approximate the interaction potential as

$$1/p_1 = 1/|x_1 - x_2| - 1/|x_1 - x_3| \quad (49)$$

$$1/p_2 = 1/|x_1 - x_2| \quad (50)$$

Obviously, on p_1 surfaces the interaction potential acting at the first particle is a constant, on p_2 surfaces the interaction potential does not depend on the position of the 3rd particle. Differences between these types of surfaces is illustrated in Fig.3. Two points' locations presented in Fig.3 determine two different surfaces for p_t because they have different value of $|x_2 - x_3|$; the same surface for p_1 because $|x_1 - x_2|$ and $|x_1 - x_3|$ is the same for both locations. These locations belong to the same surface for p_2 also; moreover, the change of the 3rd particle location does not lead to the change of the surface.

The exact diagonalization of matrix H gives 120 states belonging to the pure symmetric representation of the permutation group (not suitable for electrons), 56 to the pure antisymmetric, and 336 to the mixed symmetric (neither pure symmetric nor pure antisymmetric) representation of the permutation group.

The energies of the four lowest states obtained with CI method, and with different approximations of CWF for different n_f are shown in Table II.

The results show that for the complete basis of one-body functions $n_f = 8$ the results of the applied methods of solution give exactly the same results. In all cases, the diagonalized matrices are of the same n_f^3 order providing the exact values for other excited states. This situation continues in p_t and p_1 up to $n_f = 4$ for all states, and up to $n_f = 3$ for the ground state in spite of one-body basis set reduction. The result is a sequent that up to $n_f = 4$ the number of linear independent function constructed for p_t and p_1 surfaces remains unchanged and equals to 512. The ground state is symmetric and does not contains the exchange hole, so correlations effect here

Table II. Convergence with basis set increase for ground (g) and 1st, 2nd, and 3rd excited states obtained with p_t , p_1 , p_2 and CI matrices.

n_f	state	p_t	p_1	p_2	CI
2	g	2.5167521	2.5523628	3.2802597	4.7233508
	1st	2.6007468	2.5630105	3.3433421	4.7233508
	2nd	2.6007468	2.5810447	3.5953573	4.9761493
	3rd	2.8993370	2.7509650	3.7269786	4.9761493
3	g	2.5164929	2.5164929	2.6297927	2.7116594
	1st	2.5624931	2.5512484	2.6779104	3.1982957
	2nd	2.5624931	2.5513833	2.6926681	3.1982957
	3rd	2.6311803	2.6246885	2.7596655	3.5842098
4	g	2.5164929	2.5164929	2.5796667	2.6802123
	1st	2.5512299	2.5512296	2.5965684	2.6803017
	2nd	2.5512299	2.5512296	2.6583777	2.6803017
	3rd	2.6246904	2.6246885	2.6678403	2.7694084
5	g	2.5164929	2.5164929	2.5560362	2.6101078
	1st	2.5512296	2.5512296	2.5705697	2.6273272
	2nd	2.5512296	2.5512296	2.6028451	2.6273272
	3rd	2.6246885	2.6246885	2.6369918	2.6596377
6	g	2.5164929	2.5164929	2.5434281	2.5722193
	1st	2.5512296	2.5512296	2.5623772	2.5938677
	2nd	2.5512296	2.5512296	2.5847363	2.5938677
	3rd	2.6246885	2.6246885	2.6308173	2.6415573
7	g	2.5164929	2.5164929	2.5304009	2.5478066
	1st	2.5512296	2.5512296	2.5569004	2.5751546
	2nd	2.5512296	2.5512296	2.5676064	2.5751546
	3rd	2.6246885	2.6246885	2.6269072	2.6336853
8	g	2.5164929	2.5164929	2.5164929	2.5164929
	1st	2.5512296	2.5512296	2.5512296	2.5512296
	2nd	2.5512296	2.5512296	2.5512296	2.5512296
	3rd	2.6246885	2.6246885	2.6246885	2.6246885

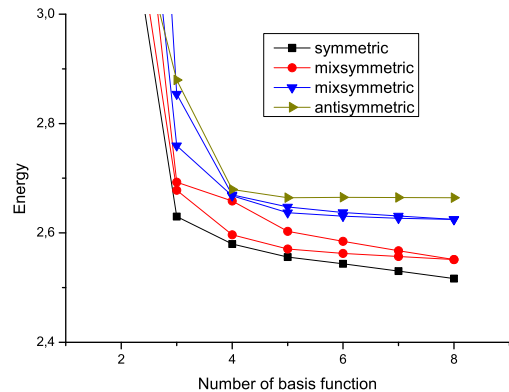


FIG. 4. Convergence with basis set increase

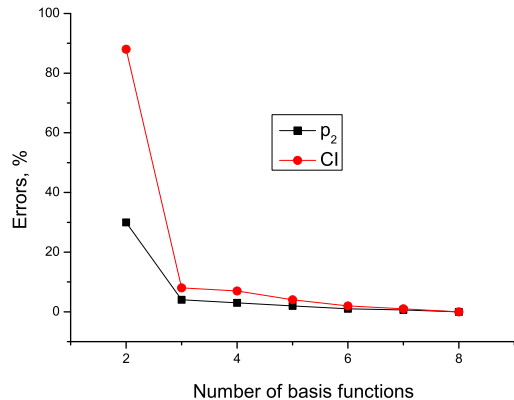


FIG. 5. Errors with basis set increase

is more important than for antisymmetric states. Other states presented in Table II are mixed symmetric.

The decrease in the number of one-bode basis functions leads to the decrease in the order of CI and p_2 matrices. As a result, the accuracy obtained with these methods drops significantly with the basis set reduction. This drop is shown in Fig. 4 for the 6 lowest states of p_2 belonging to pure symmetric, mixed symmetric and pure antisymmetric states. As one can see in Fig. 4 the loss of accuracy removes degeneration of the mixed symmetric states. Fig. 5 shows the relative errors of CI and p_2 . Approximation p_2 gives about two times less errors in comparison with CI one.

V. HE-LIKE IONS

The He-like ions has been the subject of intensive study over last decades to analyse the behavior of electrons in the nuclear field in its simplest two electron case and learn how to construct the wave function for more complicated cases.

There are several types of wave functions used in the precise electronic structure calculations of He-like ions: Hylleraas-type wave functions, conventional configuration interaction wave functions constructed from Slater-type orbitals, and configuration interaction wave functions with explicit dependence of the wave functions on r_{12} . In most calculations the Hylleraas-type wave function

$$\Psi(\mathbf{r}_1, \mathbf{r}_2) = e^{-\alpha(r_1+r_2)} \sum_{i=1}^l c_i f_i(r_1, r_2, r_{12}) \quad (51)$$

where in pioneering works of Hylleraas^{29,37} function $f_i(r_1, r_2, r_{12})$ has the form

$$f_i^H(r_1, r_2, r_{12}) = (r_1 + r_2)^{l_i} (r_1 - r_2)^{2m_i} r_{12}^{n_i} \quad (52)$$

Frankowski and Pektetis³⁸ proposed another form for $f_i(r_1, r_2, r_{12})$

$$f_i^{FP}(r_1, r_2, r_{12}) = f_i^H(r_1, r_2, r_{12}) \times [(r_1 + r_2)^2 + (r_1 - r_2)^2]^{l_i/2} [\ln(r_1 + r_2)]^{k_i} \quad (53)$$

multiplying f_i^H by the logarithmic function. The double basis function method with generalized Hylleraas functions

$$\Psi(\mathbf{r}_1, \mathbf{r}_2) = e^{-\alpha_a r_1 - \beta_a r_2} \sum_{ijk} c_{ijk}^a r_1^i r_2^j r_{12}^k + e^{-\alpha_b r_1 - \beta_b r_2} \sum_{ijk} c_{ijk}^b r_1^i r_2^j r_{12}^k \quad (54)$$

was used in.³⁹ In works⁴⁰⁻⁴³ the functions represented in the form

$$\Psi(\mathbf{r}_1, \mathbf{r}_2) = (1 + P_{12}) \sum_i a_i e^{-\alpha_i r_1 - \beta_i r_2 - \gamma_i r_{12}} \quad (55)$$

where P_{12} is the operator permuting r_1 and r_2 . These functions contain more than one nonlinear variational parameters in the exponent and up to several hundred coefficients c_i .

All applications of Hylleraas-type wave functions to He give the energy of the ground state -2.9037236 a.e. and employment of more exact functions lead to the increase in the number of significant decimal points.

Conventional configuration interaction wave functions

$$\Psi(\mathbf{r}_1, \mathbf{r}_2) = \sum_i c_i \Phi_i(\mathbf{r}_1, \mathbf{r}_2), \quad (56)$$

where Φ_i is a determinant function constructed from i set of Slater spin-orbitals, have been used for He-like ions calculations in Ref.⁴⁴. An increase in the number of nonlinear parameters allowed to reduce the expand length of configuration interaction wave function. Including an explicit dependence of a configuration interaction function on electron separation r_{12} leads to a further decrease in the wave function expand length^{40,45,46}. Obviously, the application of the theory to solve the Schrödinger equations for He-like ions has a particular importance.

Equations.

When solving the Schrödinger equations for He-like ions, for length and energy it is convenient to use the corresponding atomic units divided by nuclear charge Z and Z^2 , respectively. In these units the Schrödinger equation for 1S_0 state of He-like ions can be written in the form

$$H\Psi = \left[-\frac{1}{2} \left(\frac{\partial^2}{\partial r_1^2} + \frac{\partial^2}{\partial r_2^2} \right) - \frac{1}{r_1} \frac{\partial}{\partial r_1} - \frac{1}{r_2} \frac{\partial}{\partial r_2} - \frac{1}{r_1} - \frac{1}{r_2} + \frac{1}{Zp} \right] \Psi(r_1, r_2) = E\Psi(r_1, r_2) \quad (57)$$

where $p = |\mathbf{r}_1 - \mathbf{r}_2|$. Let us represent a many-electron wave function in the form

$$\Psi(\mathbf{r}_1, \mathbf{r}_2) = \sum_i \chi_i(p) \Phi_i(\mathbf{r}_1, \mathbf{r}_2). \quad (58)$$

where function Φ is a symmetrized production of two one-electron functions, and the weight function χ_i depends only on the total electron-electron interaction potential.

The set of equations for function χ_i can be written in the form

$$\sum_j \left[-\frac{t_{ij}(p)}{2} \frac{d^2 \chi_j(p)}{dp^2} - \frac{1}{2} \left(\frac{2t_{ij}(p)}{p} + u_{ij}(p) \right) \frac{d\chi_j(p)}{dp} + \left(h_{ij}(p) + \frac{s_{ij}(p)}{Zp} \right) \chi_j(p) \right] = E \sum_j s_{ij}(p) \chi_j(p), \quad (59)$$

with

$$s_{ij}(p) = \langle \Phi_i(\mathbf{r}_1, \mathbf{r}_2) | \Phi_j(\mathbf{r}_1, \mathbf{r}_2) \rangle_p \quad (60)$$

$$t_{ij}(p) = 2s_{ij}(p), \quad (61)$$

$$u_{ij}(p) = \langle \Phi_i(\mathbf{r}_1, \mathbf{r}_2) | \sum_{k=1}^2 \nabla_k p \nabla_k | \Phi_j(\mathbf{r}_1, \mathbf{r}_2) \rangle_p \quad (62)$$

$$= \langle \Phi_i(\mathbf{r}_1, \mathbf{r}_2) | \left. \frac{p^2 + r_1^2 - r_2^2}{2pr_1} \frac{\partial}{\partial r_1} \right| \Phi_j(\mathbf{r}_1, \mathbf{r}_2) \rangle_p, \quad (63)$$

$$+ \frac{p^2 - r_1^2 + r_2^2}{2pr_2} \frac{\partial}{\partial r_2} \Big| \Phi_j(\mathbf{r}_1, \mathbf{r}_2) \rangle_p, \quad (64)$$

$$h_{ij}(p) = \langle \Phi_i(\mathbf{r}_1, \mathbf{r}_2) | H_0(\mathbf{r}_1, \mathbf{r}_2) | \Phi_j(\mathbf{r}_1, \mathbf{r}_2) \rangle_p, \quad (65)$$

H_0 is the Hamiltonian of non-interacting electrons and averaging over space coordinates is performed for constant particle separation p . Representing $r_2 = \sqrt{r_1^2 + p^2 - 2r_1 p \cos \vartheta}$ integration over sphere of radius p with the center at r_1 can be transformed into integration over r_2

$$\int p \sin \vartheta d\vartheta d\phi = \frac{2\pi}{r_1 p} \int_{|r_1-p|}^{r_1+p} r_2 dr_2 \quad (66)$$

and matrix elements of operator \hat{F} over the whole constant interaction potential was performed as

$$F_{ij}(p) = \int dr_1 r_1^2 \int_{|r_1-p|}^{r_1+p} \frac{r_2}{pr_1} dr_2 \Phi_i(r_1, r_2) |F(r_1, r_2)| \Phi_j(r_1, r_2) \quad (67)$$

For description of 1S_0 states we will use $1s$, $2s$, $3s$ and $4s$ wave functions of an electron in the nuclear field written below

$$\begin{aligned} \phi_1(\mathbf{r}) &= 2e^{-r} \\ \phi_2(\mathbf{r}) &= \frac{1}{\sqrt{2}} \left(1 - \frac{r}{2} \right) e^{-r/2} \\ \phi_3(\mathbf{r}) &= \frac{2}{\sqrt{27}} \left(1 - \frac{2r}{3} + \frac{2r^2}{27} \right) e^{-r/3} \\ \phi_4(\mathbf{r}) &= \frac{1}{4} \left(1 - \frac{3r}{4} + \frac{r^2}{4} - \frac{r^3}{192} \right) e^{-r/4} \end{aligned} \quad (68)$$

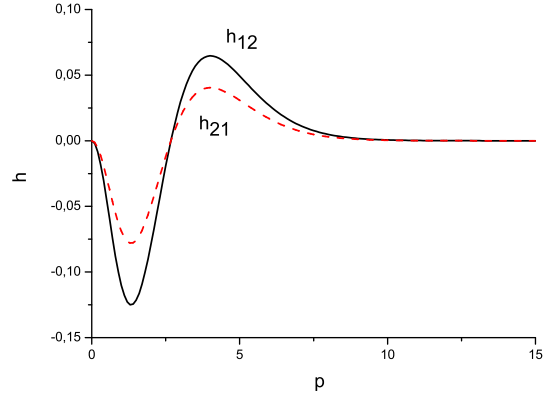


FIG. 6. H_{12} and H_{21} matrix elements

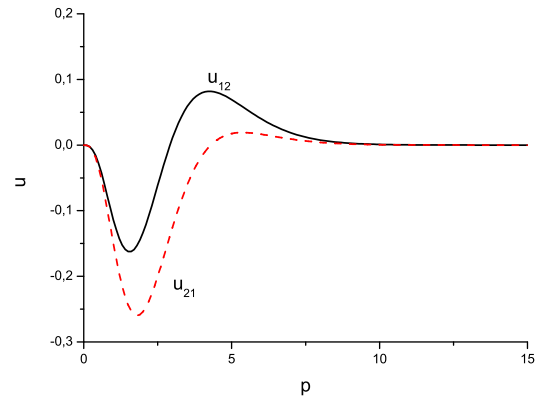


FIG. 7. U_{12} and U_{21} matrix elements

From these functions four configurations with the lowest energies will be used

$$\Phi_i(r_1, r_2) = [\phi_1(r_1)\phi_i(r_2) + \phi_1(r_2)\phi_i(r_1)] / \sqrt{2(\delta_{1i} + 1)} \quad (69)$$

Matrix elements between these functions on a surface p can be obtained analytically and presented in Appendix where one can see that the expressions for matrix elements between Φ_3 and Φ_4 functions contain very large numbers, and to avoid undesirable rounding errors the calculations were performed with 32 significant numerals.

Overlap matrix $S(p)$ is symmetric, while matrices H and U are non-symmetric. Differences in matrix elements H_{12} , H_{21} and U_{12} , U_{21} are shown in Fig. 6 and Fig. 7 respectively. The diagonal overlap matrix elements are shown in Fig. 8. Note that orthogonal functions in the whole space (69) become non-orthogonal on the constant interaction potential surface. Off-diagonal matrix elements decay with p growing faster than the diagonal ones

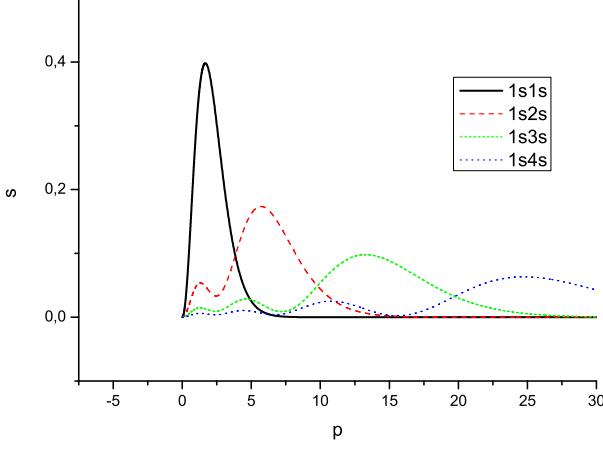


FIG. 8. Diagonal overlap matrix elements.

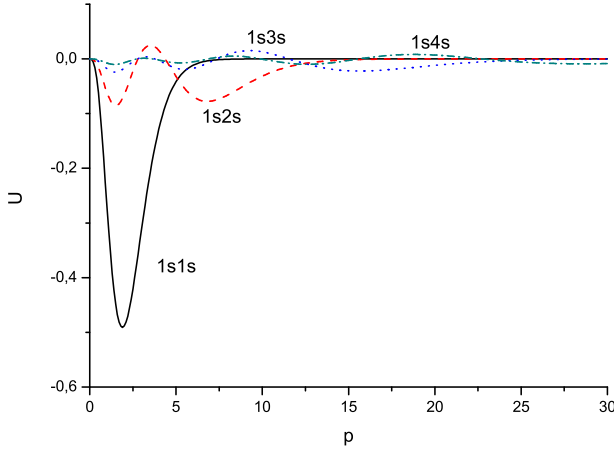


FIG. 9. Diagonal U matrix elements.

what has an important consequence - in $p \rightarrow \infty$ limit the set (13) is split into independent equations. The diagonal matrix elements of U is shown in Fig. 9. One can see in Fig.8 and Fig.9 that both matrix elements S and U decay with p growth, however not too fast to neglect them in a precise calculations for rather big p .

The Hamiltonian matrix elements of non-interacting electrons reduced to

$$h_{ij} = \epsilon_j s_{ij} \quad (70)$$

where ϵ_j is the energy of Φ_j state. Due to ϵ_j factor $h_{ij}(p) \neq h_{ji}(p)$. Naturally, in the whole space non-diagonal elements obtained by integration over p equal to zero and matrix h become Hermitian.

Boundary conditions and computation details.

The boundary conditions for χ follow from the demand for Ψ to be finite in the whole space

$$\chi_i(p) s_{ij}(p) \chi_j(p) < \infty, \quad i, j = 1, \dots, n_f, \quad (71)$$

n_f is the size of basis set used. Series expansion of U matrix elements shows that $u_{ij} \rightarrow cp^3$ when $p \rightarrow 0$, i.e. u_{ij} decay faster than s_{ij} elements with $p \rightarrow 0$. Thus, for small p Eqs.(59) can be approximated by equation

$$2 \frac{d\omega}{dp} + \frac{\omega}{Z} = 0 \quad (72)$$

with solution

$$\omega(p) = e^{Zp/2} \quad (73)$$

Determine the general solutions of (59) as

$$\chi^l(p, E) = \sum_i c_i^l \chi_i^l(p, E) \quad (74)$$

where c_i^l are arbitrary constants and $\chi_i^l(p, E)$ is partial solution of (59) with the initial values

$$\chi_i^l(0) = \omega(0) \sum_j \delta_{ij} \quad (75)$$

$$\frac{d\chi_i^l(0)}{dp} = \frac{Z}{2} \chi_i^l(0) \quad (76)$$

The superscript l means that χ^l are determined from the left initial values, each χ_i^l is a vector function.

To defined the boundary condition when $p \rightarrow \infty$, we represent the solution of (59) at a point p as $e^{\lambda p}$. Substitution of this representation in (59) leads to

$$\sum_{j=1}^n [-\lambda^2 s_{ij}(p) - \lambda((2s_{ij}(p)/p + u_{ij}(p)) + h_{ij}(p)) + s_{ij}(p)/Zp - E s_{ij}(p)] \chi_j(p) = 0, \quad i = 1, \dots, n_f, \quad (77)$$

Set (77) has non-zero solution if

$$\det(\Lambda) = 0 \quad (78)$$

where matrix Λ is determined by the expressions in the square brackets of (77). Obviously, $\det(\Lambda)$ is a $2n_f$ order polynomial of λ the $2n_f$ roots of which, possibly complex, will be denoted λ_i . Not all of the roots satisfy the condition (71). In particular, for $n_f = 1$ taking into account that $u_{11}/s_{11} \rightarrow -2$ when $p \rightarrow \infty$, the two roots of (78) in this limits are

$$\lambda_{1,2} = 1 \pm \sqrt{1 + \epsilon_1 - E} \quad (79)$$

Function χ satisfies to the condition (71) only for λ_2 . It is a growing function for $E > \epsilon_1$ and a decreasing one for $E < \epsilon_1$. For $E = \epsilon_1$ $\lambda_2 = 0$ and the configuration

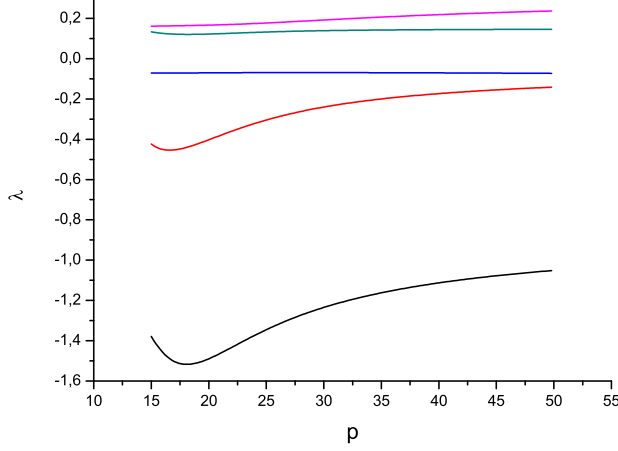


FIG. 10. Roots of (24) satisfying to (71) as a function of p for $n_f = 4$. Physical meaning have the four lowest roots.

weight function becomes a constant as it should be for non-interaction electrons.

For $n_f = 4$ the dependence on p of the roots satisfying condition (71) is shown in Fig.10. Determine partial solutions of (13) $\chi_i^r(p, E)$ which satisfy boundary conditions

$$\begin{aligned} \chi_i^r(p, E) &= e^{\lambda p} \\ \frac{d\chi_i^r(p, E)}{dp} &= \lambda_i \chi_i^r(p, E) \end{aligned} \quad (80)$$

The general solution of (13) with these right boundary conditions can be presented in the form

$$\chi^r(p, E) = \sum_i^n c_i^r \chi_i^r(p, E) \quad (81)$$

Coefficients c^l and c^r are determined from the demand that functions χ_i^l must continuously pass to functions χ_i^r at a point p together with their 1st derivatives

$$\chi_i^l(p, E) = \chi_i^r(p, E) \quad (82)$$

$$\frac{\chi_i^l(p, E)}{dp} = \frac{\chi_i^r(p, E)}{dp} \quad (83)$$

For solubility of this set of equation it is necessary that

$$\det(\Omega(E)) = 0 \quad (84)$$

where

$$\Omega = \begin{vmatrix} \chi^l(p, E) & -\chi^r(p, E) \\ \frac{\chi^l(p, E)}{dp} & -\frac{\chi^r(p, E)}{dp} \end{vmatrix} \quad (85)$$

Condition (84) determines the energy E of the system.

To solve (59) for $n_f < 4$ with the boulder condition (75) or (80) the Runge-Kutta 4th-order method can be employed. For $n_f = 4$ equations (59) become stiff and it is impossible to obtain solution with Runge-Kutta method due to fast growth of rounding errors leads to divergence of the searching solution. Described in⁴⁷ Rosenbrock method elaborated for stiff equations also failed to solve the problem. We succeed in solving (59) exploiting tridiagonal matrix algorithm (Thomas algorithm)⁴⁸. For these equations (59) were approximated with

$$\mathbf{A}_k \chi(k-1) + \mathbf{B}_k \chi(k) + \mathbf{C}_k \chi(k+1) = 0 \quad (86)$$

Here k numerates points of p -mesh,

$$\mathbf{A}_k = -2\mathbf{t}_k/d^2 + (\mathbf{h}_k/p_k + \mathbf{u}_k/2)/d \quad (87)$$

$$\mathbf{C}_k = -2\mathbf{t}_k/d^2 - (\mathbf{s}_k/p_k + \mathbf{u}_k/2)/d \quad (88)$$

$$\mathbf{B}_k = \mathbf{h}_k + (q/p_k - E)\mathbf{s}_k \quad (89)$$

$d = p_{k+1} - p_k$, \mathbf{t} , \mathbf{u} , \mathbf{h} and \mathbf{s} are $n_f \times n_f$ matrices, χ is n_f -order vector.

In line with the Tomas algorithm partial solutions of (86) can be represented as

$$\chi_i(k) = \mathbf{X}_{ik}^l \chi(k+1), \quad i = 1, \dots, n_f \quad (90)$$

where matrix

$$\mathbf{X}_{ik}^l = -(\mathbf{A}_k \mathbf{X}_{i,k-1}^l + \mathbf{B}_k)^{-1} \mathbf{C}_k \quad (91)$$

with

$$\mathbf{X}_{i,0}^l = e^{-Zd/2} \delta_{ij}, \quad j = 1, \dots, n_f \quad (92)$$

The choice of \mathbf{X}_0^l follows from (76) and determines the correct 1st derivatives of the function rather than the function values. Thus the solution of (86) is through the calculation of \mathbf{X}^l with (91) in upward direction at the first stage and the calculation of χ with (90) in backward direction.

Obviously the algorithm can be reversed, i.e. the calculation of \mathbf{X}^r starting from a big p and calculate χ in the backward direction. Corresponding formulas for a partial solution are presented below

$$\chi_i^r(k+1) = \mathbf{X}_{ik}^r \chi_i(k), \quad i = 1, \dots, n_f \quad (93)$$

$$\mathbf{X}_{i,k-1}^r = (\mathbf{A}_k \mathbf{X}_{ik}^r + \mathbf{B}_k)^{-1} \mathbf{C}_k \quad (94)$$

$$\mathbf{X}_{in}^r = e^{\lambda_i d} \delta_{ij} \quad i = 1, \dots, n_f \quad (95)$$

λ_i are roots of (78). (95) provides boulder conditions for a partial solution of (86) for big p .

In principle, one can use to solve (86) formulas (90)-(92) or (93)-(95). However, computational errors can grow with moving off the border. To decrease these errors, it is useful to apply both of these ways, matching their solution at some point inside p -interval. At this point functions χ_i and their 1st derivatives calculated

with \mathbf{X}^l and \mathbf{X}^r must be equal to each other. The derivatives can be presented in the forms

$$\chi'_i(m) = (\mathbf{I} - \mathbf{X}_{im}^l)\chi_i(m)/d \quad (96)$$

$$\chi'_i(m) = (-\mathbf{I} + \mathbf{X}_{im}^r)\chi_i(m)/d \quad (97)$$

The matching conditions lead to a set of equations

$$\sum_i \chi_i^l(m)c_i^l = \sum_i \chi_i^r(m)c_i^r \quad (98)$$

$$\sum_i (\mathbf{I} - \mathbf{X}_{i,m-1}^l)c_i^l = \sum_i (\mathbf{I} - \mathbf{X}_{i,m+1}^r)\chi_i(m)c_i^r$$

The set of equations (98) determined the system energy because the set has nonzero solution only for selected energies making the determinant of the set equals to zero. As seen in Fig.10 $\lambda_i(p)$ tends to constant when $p \rightarrow \infty$ and a use of finite p introduce an errors in to the calculated energy. From the other side, the numerical errors tends to grows for too large p . In energy calculations we used $p = 40$. This value is a compromise between the variation of λ_4 and the increasing numerical errors with p growth.

Results.

The energies obtained with (59) for the ground states of He-like ions are presented in Table I together with HF and configuration interaction results. The use of only one configuration in (58) gives energies slightly below Hartree-Fock limit. Inclusion 2nd and 3rd configurations gives the results comparable but slightly above those of CI with 35 configurations. When the fourth configuration is added, the energies fall below the CI results and below Hylleraas limit excepting of O^6 .

The configuration weight functions H^-, \dots, Ar^{16+} for one-configuration approximation are shown in Fig.11. The H^- configuration weight function demonstrates the most rapid growth with p . The functions growth slow down with the increase in nuclear charges and tends to a constant, demonstrating a relative decrease in electron-electron interaction as compared to the nuclear field. The growing interaction function decreases the probability to find electron at a small separation and increase at a bigger separation in comparison with non-interacting cases.

The configuration weight functions from He to Ar^{16+} for even atomic numbers are shown in Fig.12. As one can see $1s1s$ configuration weights are similar to the configuration weight functions for $n_f = 1$ (see Fig.11). The $1s2s$ functions have noticeable values for small p which tends decrease with the growth of p and the atomic number.

The configuration weight functions of He and Ar^{16+} for 3-configuration approximation are shown in Fig.13 and Fig.14, correspondingly. It can be seen that the absolute value of $1s3s$ weight function for He in small p region significantly exceeds the approximately equal

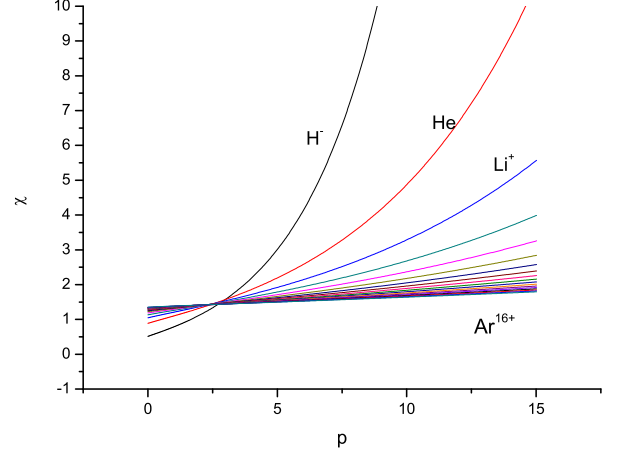


FIG. 11. Configuration wave functions of H^-, \dots, Ar^{16+} for $1s1s$ configuration approximation.

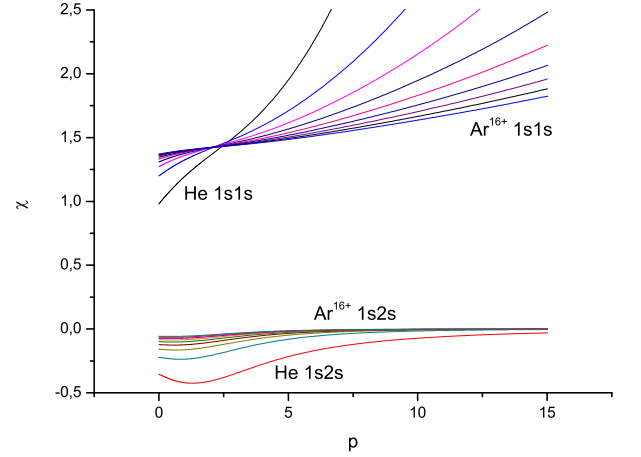


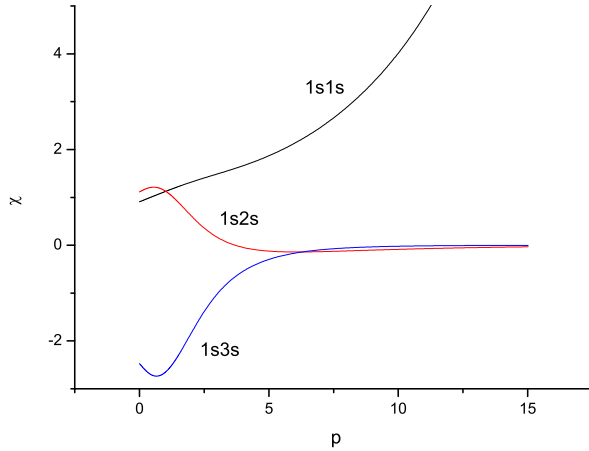
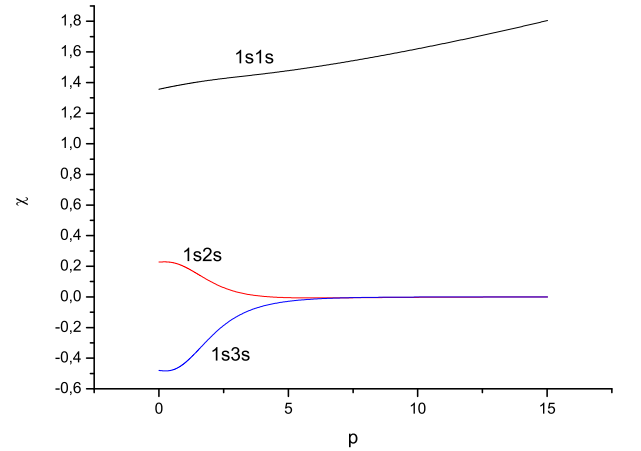
FIG. 12. $1s1s$ and $1s2s$ configurations wave functions from He to Ar^{16+} for even atomic numbers for 2-configuration approximation.

contributions of $1s1s$ and $1s2s$ configurations, with the growth of p contribution $1s1s$ dominating. When nuclear charge increases the contributions of $1s2s$ and $1s3s$ configurations tend to decrease. The weight functions for Ar^{16+} are similar to those for He ; however, the relative contribution of $1s2s$ and $1s3s$ to the wave function decreases in comparison with $1s1s$ contribution.

The configuration weight functions for He with $n_f = 4$ are shown Fig.15. The contribution of $1s1s$, $1s2s$ and $1s3s$ interact weight function into the wave function are similar $n_f = 3$ case; however, a peak and a visible knee close to $p = 2.6$ appear at the $1s2s$ and $1s3s$ weight func-

TABLE I. The ground states energies of He-like ions.

Ion	Energy, a.u.							
	HF ^a	1	2	3	4	CI ^b	Hyl ^c	Exp. ^d
H^-		-0.498461	-0.526779	-0.527133	-0.527790	-0.5277303		
He	-2.86171	-2.879388	-2.900539	-2.902257	-2.903756	-2.9037236	-2.903724	-2.90338
Li^+	-7.23633	-7.256393	-7.276105	-7.278158	-7.279468	-7.279819	-7.279913	-7.278956
Be^{2+}	-13.61130	-13.632404	-13.651487	-13.653685	-13.655578	-13.655551	-13.655566	-13.6574
B^{3+}	-21.98607	-22.008016	-22.026751	-22.029031	-22.031332	-22.030875	-22.030972	-22.0360
C^{4+}	-32.36137	-32.383429	-32.401946	-32.404281	-32.407322	-32.406070	-32.406247	-32.4174
N^{5+}	-44.73618	-44.758728	-44.777098	-44.779475	-44.781458	-44.781141	-44.781445	-44.8035
O^{6+}	-59.11159	-59.133956	-59.152223	-59.154631	-59.156576	-59.156222	-59.156595	-59.1958
F^{7+}	-75.48702	-75.509136	-75.527329	-75.529764	-75.532249	-75.531401	-75.531712	-75.54413
Ne^{8+}	-93.86174	-93.884283	-93.902421	-93.904878	-93.910240	-93.906452	-93.906807	-94.0086
Na^{9+}		-114.259406	-114.277503	-114.279981	-114.283217	-114.28165		
Mg^{10+}		-136.634511	-136.652577	-136.655073	-136.659456	-136.65672		
Al^{11+}		-161.009602	-161.027646	-161.030158	-161.044494	-161.03180		
Si^{12+}		-187.384681	-187.402709	-187.405237	-187.412848	-187.40687		
P^{13+}		-215.759753	-215.777769	-215.780312	-215.78715	-215.78191		
S^{14+}		-246.134816	-246.152826	-246.155383	-246.159333	-246.15697		
Cl^{15+}		-278.509875	-278.527880	-278.530450	-278.535628	-278.53201		
Ar^{16+}		-312.884928	-312.902932	-312.905515	-312.913206	-312.90704		

^a Ref.⁴⁹.^b Ref.⁴⁶.^c Ref.⁵⁰^d Ref.^{51,52}FIG. 13. He configuration wave function for $n_f = 3$.FIG. 14. Ar^{16+} configuration wave functions for $n_f = 3$.

tions. The absolute value of $1s4s$ contribution is comparable with $1s1s$ contributions and reaches a maximum close to $p = 2.6$ and then drops down.

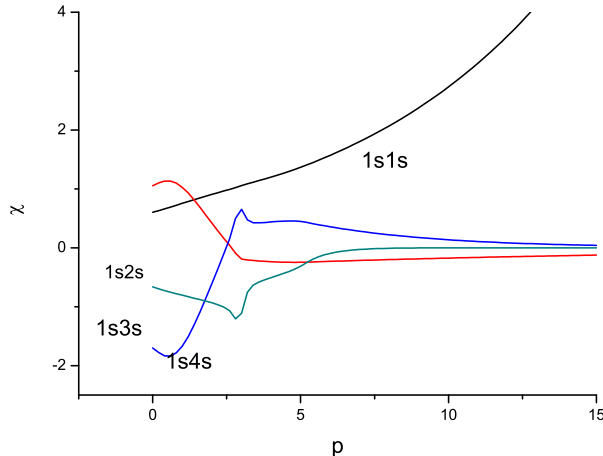


FIG. 15. *He* configuration wave functions for $n_f = 4$.

VI. CONCLUSIONS

The proposed theory can be considered as an extension of configuration interaction method in which contributions of different configurations to the wave function become dependent on the values of interaction potential, which makes the wave function more flexible and eliminates the influence of the wave function cusps on the convergence of the wave function to the exact one with a basis set increase. From the other side, the theory can be compared with explicitly correlated *R12* and *F12* methods since coefficients of wave function expansion over configurations depend on the inter particle separations and can be considered as a kind of wave function factors explicitly depending on a particle-particle separation. The main difference between these theories is the form of dependence of these factors on particle-particle separation which, in explicitly correlated theories, is prescribed whereas in the presented theory the factors are obtained by the solution of the corresponding weight function equations (13).

Equations (13) were developed by energy variation, therefore, they provide upper bounds to the ground-state energy.

The important future of the proposed method, as opposed to common methods of electronic structure calculations, is employing a basis set of non-interacting particle which does not presupposed the use of iteration procedure of Hartree-Fock method.

The solution of model examples proves that the theory is correct. The energies obtained with approximations to the theory are greater than the exact ones and converged to the exact results, so these approximations satisfy the variational principle. The convergence of CWF method with basis set increase even in its lowest approximation is faster than that of CI method.

The performed calculations show that the developed theory in the lowest approximation with only one configuration of non-interacting particles gives energies of He-like ions below the Hartree-Fock limits. The use of three configurations constructed from *1s*, *2s*, and *3s* wave functions of non-interacting electrons in the nuclear field gives ground state energies of He-like ions close to configuration interaction wave function with 35 configurations constructed from seven *s*, *p*, *d*, *f*, and *g* Slater type orbitals and with configuration interaction wave function with 15 configuration constructed from 5 Slater orbitals and explicit r_{12} terms up to the 5th order. Addition of the 4th configuration with *4s* functions gives the energies below the CI method and the Hylleraas limit. The results were obtained without iteration procedure of self-consistent field because the developed theory does not presuppose the use of the Hartree-Fock approximation as a preliminary step for precise calculations.

The equations (13) were obtained by energy variation and their application to the solution of the simple model shows that such equations do not contradict the variational principle, so the reasons why the obtained energies with $n_f = 4$ turn out to drop below the most precise calculations should be sought elsewhere. Most probably the numerical calculations has been performed with insufficient accuracy. We used direct numerical solutions of (13). If for $n_f < 4$ the application of the Runge-Kutta algorithm makes it possible to perform the calculations with a given accuracy, whereas for $n_f = 4$ this algorithm does no work since the equations become too stiff and numerical errors become unacceptable. Moreover, the application of the Rosenbrock method for solving stiff equations also failed to solve the problem. The Thomas algorithm used in this work significantly reduced the numerical errors, however it needs improving to guarantee the desired accuracy. Another way to solve (13) is to search the solutions in the form of a linear combination of some basis functions as it was done in all precise methods. In this case one has to find a basis which will be complete and fast converging.

It should be noted that any expansion of the theory on many-atomic systems presupposes the construction of molecular orbitals of non-interacting electrons. It is these orbitals that should be used in averaging of one-bode operators over interaction potential surfaces, whereas surfaces themselves do not depend on nuclear positions.

ACKNOWLEDGMENTS

The author gratefully acknowledges helpful discussions with the colleagues from Laboratory of Quantum Chemistry of Boreskov Institute of Catalysis.

¹C. D. Sherrill, *The Journal of Chemical Physics* **132**, 110902 (2010).

²T. Kato, *Communications on Pure and Applied Mathematics* **10**, 151 (1957).

- ³H. King, *Theor. Chim. Acta* **94**, 345 (1996).
- ⁴P. Hohenberg and W. Kohn, *Physical Review* **136**, B864 (1964).
- ⁵W. Kohn and L. J. Sham, *Physical Review* **140**, A1133 (1965).
- ⁶P. Hohenberg and W. Kohn, *J. Phys. Chem.* **100**, 12974 (1996).
- ⁷C. Christopher and D. Truhlar, *Phys. Chem. Chem. Phys.* **11**, 10757 (2009).
- ⁸N. Ivanova, S. Ovchinnikov, M. Korshunov, I. Eremin, and N. Kazak, *Physics-Uspekhi* **179**, 837 (2009).
- ⁹F. Lechermann, A. Georges, A. Poteryaev, S. Biermann, M. Posternak, A. Yamasaki, and O. K. Andersen, *Phys. Rev. B* **74**, 125120 (2006).
- ¹⁰E. Dagotto, *Science* **309**, 257 (2005).
- ¹¹W. Kutzelnigg and W. Klopper, *The Journal of Chemical Physics* **94**, 1985 (1991).
- ¹²W. Klopper, *Chemical Physics Letters* **186**, 583 (1991).
- ¹³V. Termath, W. Klopper, and W. Kutzelnigg, *The Journal of Chemical Physics* **94**, 2002 (1991).
- ¹⁴J. Noga, W. Kutzelnigg, and W. Klopper, *Chemical Physics Letters* **199**, 497 (1992).
- ¹⁵J. Noga and W. Kutzelnigg, *The Journal of Chemical Physics* **101**, 7738 (1994).
- ¹⁶J. Noga and P. Valiron, *Chemical Physics Letters* **324**, 166 (2000).
- ¹⁷E. F. Valeev and H. F. S. III, *The Journal of Chemical Physics* **113**, 3990 (2000).
- ¹⁸W. Klopper and C. C. M. Samson, *The Journal of Chemical Physics* **116**, 6397 (2002).
- ¹⁹W. Klopper, *The Journal of Chemical Physics* **120**, 10890 (2004).
- ²⁰E. F. Valeev, *Chemical Physics Letters* **395**, 190 (2004).
- ²¹S. Ten-no, *Chemical Physics Letters* **398**, 56 (2004).
- ²²E. F. Valeev, *The Journal of Chemical Physics* **125**, 244106 (2006).
- ²³T. Shiozaki, E. F. Valeev, and S. Hirata, *The Journal of Chemical Physics* **131**, 44118 (2009).
- ²⁴M. Torheyden and E. F. Valeev, *The Journal of Chemical Physics* **131**, 171103 (2009).
- ²⁵K. A. Peterson, T. B. Adler, and H.-J. Werner, *The Journal of Chemical Physics* **128**, 84102 (2008).
- ²⁶K. E. Yousaf and K. A. Peterson, *Chemical Physics Letters* **476**, 303 (2009).
- ²⁷W. Klopper, F. R. Manby, S. Ten-no, and E. F. Valeev, *Int. Rev. Phys. Chem* **25**, 427 (2006).
- ²⁸C. Hättig, W. Klopper, A. Köhn, and D. P. Tew, *Chemical Reviews* **112**, 4 (2012), <http://pubs.acs.org/doi/pdf/10.1021/cr200168z>.
- ²⁹E. Hylleraas, *Z. Phys.* **54**, 347 (1929).
- ³⁰E. Hylleraas, *Z. Phys.* **65**, 209 (1930).
- ³¹S. Boys and N. Handy, *Proc. Roy. Soc. A* **309**, 209 (1969).
- ³²S. Boys and N. Handy, *Proc. Roy. Soc. A* **310**, 43 (1969).
- ³³H. Nakatsuji, *Phys. Rev. Lett.* **93**, 030403 (2004).
- ³⁴H. Nakatsuji, *Phys. Rev. A* **72**, 062110 (2005).
- ³⁵V. Tapilin, *J. Struct. Chem.* **49**, 409 (2008); **58**, 1 (2017).
- ³⁶L. Landau and L. Lifshits, *Quantum Mechanics: Non-Relativistic Theory* (Pergamon, London, 1977).
- ³⁷E. Hylleraas, *Z. Phys.* **48**, 469 (1928).
- ³⁸K. Frankowski and C. L. Pekeris, *Phys. Rev.* **146**, 46 (1966).
- ³⁹G. W. F. Drake and Z.-C. Yan, *Chem. Phys. Lett.* **229**, 486 (1994).
- ⁴⁰A. J. Thakkar and V. H. Smith, *Phys. Rev. A* **15**, 1 (1977).
- ⁴¹A. J. Thakkar and V. H. Smith, *Phys. Rev. A* **15**, 16 (1977).
- ⁴²A. S.A. and M. H.j., *Phys. Rev. A* **38**, 26 (1988).
- ⁴³V. Korobov, *Phys. Rev. A* **064503**, 1 (2017).
- ⁴⁴A. Weiss, *Phys. Rev.* **122**, 1826 (1961).
- ⁴⁵C. Roothaan and A. Weiss, *Revs. Modern Phys.* **32**, 194 (1960).
- ⁴⁶B. Saha, S. Bhattacharyya, T. K. Mukherjee, and P. K. Mukherjee, *Int. J. Quantum Chem.* **92**, 413 (2003).
- ⁴⁷W. Press, W. Tenkolsky, S.A. and Vetterling, and B. Flannery, *Numerical Recipes in Fortran 90: The Art of Parallel Scientific Computing* (University Press, Cambridge, 2002) p. 727.
- ⁴⁸N. Yanenko, *The method of fractional steps (The solution of problems of mathematical physics in several variables)* (Springer-Verl., Berlin, 1971).
- ⁴⁹E. Clementi and C. Roetti, *Atomic data and Nuclear data Tables* **14**, 177 (1974).
- ⁵⁰A. J. Thakkar and T. Koga, *Phys. Rev. A* **50**, 854 (1994).
- ⁵¹C. Moore, *Atomic Energy Levels*, Vol. 1 (NSRDS-NBS 35, 1971).
- ⁵²S. Bashkin and J. Stoner, Jr., *Atomic Energy Levels and Grottrian Diograms*, Vol. I and II (North-Holland, Amsterdam, 1975, 1978).